O-Alkyl-5',5'-dinucleoside Phosphates as Prodrugs of 3'-Azidothymidine and Cordycepin[1]

Chris Meier,[†,‡] Jean-Michel Neumann,[§] François André,[§] Yvette Henin,[⊥] and Tam Huynh-Dinh*[,†]

Unité de Chimie Organique, URA CNRS 487, Institut Pasteur, 28, Rue du Docteur Roux, 75724 Paris Cedex 15, France, Groupe de RMN, URA CNRS, 1290, CEA, Centre d'Etudes Nucléaires de Saclay, 91191 Gif-sur-Yvette, France, and Unité d'Oncologie Virale, URA CNRS 1157, Institut Pasteur, 28, Rue du Docteur Roux, 75724 Paris Cedex 15, France

Received June 5, 1992

The syntheses of two O-alkyl-5',5'-dinucleoside phosphotriesters **2a** and **2b** as combined prodrugs of the antiviral drug AZT (1) and the antibiotic agent cordycepin (3) are described. **2a,b** were obtained as a 1:1 diastereomeric mixture. The absolute configuration of the isolated diastereomers was determined by NOE NMR experiments and correlated with the migration characteristics on silica gel as well as the ^{31}P-NMR chemical shift. The conformational features of $\mathbf{2b}_R$ and $\mathbf{2b}_S$ were determined in deuteriated dodecylphosphocholine micelles in aqueous solution using 2D-NOESY spectra and shown to be dependent on the configuration at phosphorus. Additionally, all new compounds were tested for their antiviral activities in HIV-1-infected CEM C113 and H9 cell systems. Although all compounds were able to significantly inhibit the HIV-1-induced cytopathogenic effect, only the phosphodiester **12** gave a selectivity index (SI_{RT} = 2000) comparable to the reference compound AZT (1) (SI_{RT} = 3000).

Introduction

The use of nucleoside analogues in chemotherapy is one approach for the control of acquired immunodeficiency syndrome (AIDS) caused by the retrovirus HIV. After penetration through the cell membranes,[2,3] the essential steps in the mode of action of antiviral nucleosides are their conversions into the 5'-mono-, di-, and triphosphates by cellular or virus-induced kinases. The triphosphates of the nucleoside analogues act as inhibitors of the viral polymerases or as elongation terminators of the growing viral DNA chain.[4,5] The first clinical drug is 3'-azido-3'-deoxythymidine (AZT, 1)[5-7] and to circumvent its serious toxic side effects, particularly bone marrow suppression,[9] different approaches for replacement of AZT by other nucleoside analogues[10] are under current investigation.

Recently, it has been shown that a combined treatment of an antiviral and an antibiotic presented advantages with regard to single drug treatment in AIDS and the AIDS-related complex (ARC). This permits a reduction in individual doses and would decrease toxicity side effects.[11] One approach to combination therapy involves the use of dimers of antiviral nucleosides which are 5',5'-linked via a phosphate bridge,[12] but this approach does not improve the crossing of the cell membranes or the blood-brain barrier since these phosphate derivatives are charged compounds.

We have recently (i) described the synthesis of lipophilic phosphotriester of thymidine[13] and (ii) its membrane transport across unilamellar vesicles,[14] (iii) demonstrated the importance of the alkyl chain length for the drug-membrane interaction,[15] and (iv) applied these results in the synthesis of lipophilic phosphotriesters of AZT.[16] As a development of previous work, we believe that the introduction of lipophilic masked dinucleoside phosphoesters could fulfill the requirements mentioned above (prodrug approach). In this work, we report the syntheses, NMR structural analysis at a water/micelle interface (of the two diastereoisomers when isolated), and anti-HIV activities of two phosphotriesters **2a** and **2b** containing (a) 3'-azido-3'-deoxythymidine (AZT) 1,[17] (b) 3'-deoxyadenosine (cordycepin, 3) as antiviral and antibiotic nucleoside,[18] and (c) an alkyl residue (**2a**, R = C_6H_{13}, and **2b**, R = $C_{16}H_{33}$)

† Unité de Chimie Organique, Institut Pasteur.
‡ Present address: University of Frankfurt/Main, Niederurseler Hang 29, Postfach 111932, D-6000 Frankfurt/Main, FRG.
§ Centre d'Etudes Nucléaires de Saclay.
⊥ Unité d'Oncologie Virale, Institut Pasteur.

(1) Part of this work has been published as a short communication: Meier, C.; Huynh-Dinh, T. *Bioorg. Med. Chem. Lett.* **1991**, *2*, 527.
(2) AZT permeates the membranes by passive diffusion: Zimmerman, T. P.; Mahony, W. B.; Prus, K. L. *J. Biol. Chem.* **1987**, *262*, 5748.
(3) AZT crosses the blood-brain barrier: see refs 2-4 and: Klecker, R. W.; Collins, J. M.; Yarchoan, R.; Thomas, R. V.; Jenkins, J. F.; Broder, S.; Myers, C. E. *Clin. Pharmacol. Ther.* **1987**, *41*, 407.
(4) Yarchoan, R.; Klecker, R. W.; Weinhold, K. J.; Markham, P. D.; Lylerly, H. K.; Durack, D. T.; Gelman, E.; Nusinoff-Lehrman, S.; Blum, R. M.; Barry, D. W.; Shearer, G. M.; Fishi, M. A.; Mitsuya, H.; Gallo, R. C.; Collins, J. M.; Bolognesi, D.; Myers, C. E.; Broder, S. *Lancet* **1986**, *i*, 575.
(5) Heidenreich, O.; Eckstein, F. *Nucleosides Nucleotides* **1991**, *10*, 535.
(6) Mitsuya, H.; Weinhold, K. J.; Furman, P. A.; St. Clair, M. H.; Nusinoff-Lehrman, S.; Gallo, R. C.; Bolognesi, D.; Barry, D. W.; Broder, S. *Proc. Natl. Acad. Sci. U.S.A.* **1985**, *82*, 7096.
(7) Fishl, M. A.; Richman, D. D.; Grieco, M. H.; Gottlieb, M. S.; Volberding, P. A.; Laskin, O. L.; Leedom, J. M.; Groopman, J. E.; Mildvan, D.; Schooley, R. T.; Jackson, G. G.; Durack, D. T.; Phil, D.; King, D.; The AZT Collaborative Group. *N. Engl. J. Med.* **1987**, *317*, 185.
(8) Yarchoan, R.; Brouwers, P.; Spitzer, A. R.; Grafman, J.; Safai, B.; Perno, C. F.; Larson, S. M.; Berg, G.; Fishl, M. A.; Wichman, A.; Thomas, R. V.; Brunetti, A. Schmidt, P. J.; Myers, C. E.; Broder, S. *Lancet* **1987**, *i*, 132.
(9) Richman, D. D.; Fishl, M. A.; Grieco, M. H.; Gottlieb, M. S.; Volberding, P. A.; Laskin, O. L.; Leedom, J. M.; Groopman, J. E.; Mildvan, D.; Hirsch, M. S.; Jackson, G. G.; Durack, D. T.; Nusinoff-Lehrman, S.; The AZT Collaborative Group. *N. Engl. J. Med.* **1987**, *317*, 192.
(10) Mitsuya, H.; Broder, S. *Proc. Natl. Acad. Sci. U.S.A.* **1986**, *83*, 1911.
(11) Additionally, recently published results showed that the combination of an antiviral agent and an antibiotic agent may be useful in the treatment of AIDS infections: Lemaitre, M.; Guetard, D.; Henin, Y.; Montagnier, L.; Zerial, A. *Res. Virol.* **1990**, *141*, 5. Mitsuya, H.; Yarchoan, R.; Broder, S. *Science* **1990**, *249*, 1533.
(12) Hahn, E. F.; Busso, M.; Mian, A. M.; Resnick, L. In *Nucleotide Analogues as Antiviral Agents*; Martin, J. C., Ed.; ACS Symposium Series 401, American Chemical Society: Washington, DC, 1989; p 156.
(13) Iglesias-Guerra, F.; Neumann, J. M.; Huynh-Dinh, T. *Tetrahedron Lett.* **1987**, *28*, 3581.
(14) Neumann, J. M.; Herve, M.; Debouzy, J.-C.; Iglesias-Guerra, F.; Gouyette, C.; Dupraz, B.; Huynh-Dinh, T. *J. Am. Chem. Soc.* **1989**, *111*, 4270.
(15) Debouzy, J.-C.; Herve, M.; Neumann, J. M.; Gouyette, C.; Dupraz, B.; Huynh-Dinh, T. *Biochem. Pharm.* **1990**, *39*, 1657.
(16) Henin, Y.; Gouyette, C.; Schwartz, O.; Debouzy, J.-C.; Neumann, J. M.; Huynh-Dinh, T. *J. Med. Chem.* **1991**, *34*, 1830.
(17) Horwitz, J. P.; Chua, J.; Noel, M. J. *J. Org. Chem.* **1964**, *29*, 2076.
(18) Suhadolink, R. J. *Nucleosides as Biological Probes*; Wiley-Interscience & Sons: New York, 1979; pp 118-135 and references cited therein.

0022-3263/92/1957-7300$03.00/0

Scheme I

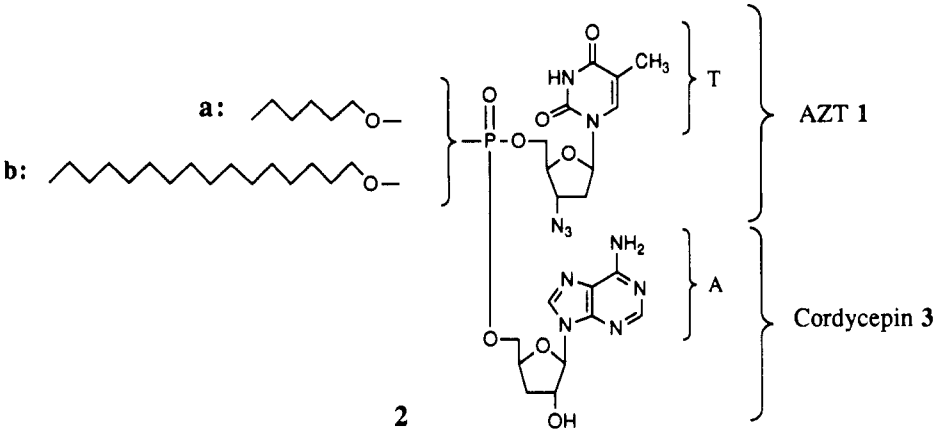

Scheme II[a]

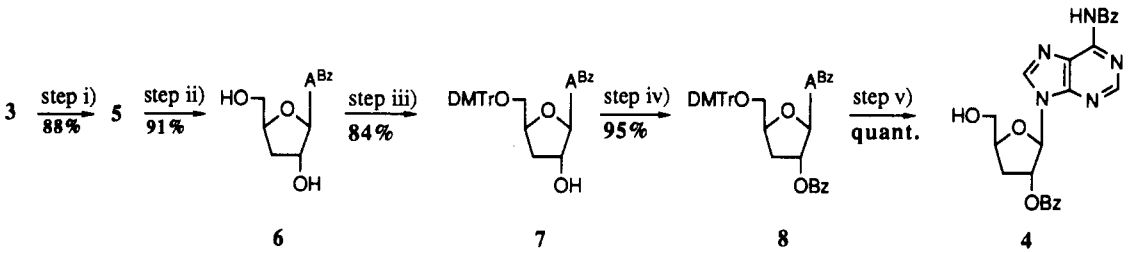

[a] Steps: (i) 6 equiv of BzCl, pyridine, 2.5 h, 0 °C;[25] (ii) 1.5 M $NaOH/H_2O$, MeOH/THf (1:1), 30 min, 0 °C;[25] (iii) 1.1 equiv of DMTrCl, pyridine, 1.1 equiv of DIPEA, 0.1 equiv of DMAP, 10 h, rt; (iv) 1.1 equiv of PhC(O)OC(O)Ph, CH_3CN, DMAP (cat.), NEt_3, 1.5 h, rt; (v) 2% BSA in CH_2Cl_2/MeOH, 10 min, rt.

esterified at the third acid group of the phosphate moiety (Scheme I).

We hypothesized that the phosphotriesters **2a** and **2b** could provide superior pharmacological properties for the following reasons: (i) the aliphatic chains facilitate the passive membrane transport of the nucleoside analogues (the two alkyl residues were chosen to investigate their effect in the lipophilicity), (ii) two different nucleoside analogues are delivered to the cell simultaneously, one as the parent nucleoside and one as its monophosphate (this is of special interest with respect to antiviral nucleosides which require intracellular kinase to convert them into 5'-nucleotides,[19] (iii) **2a** and **2b** could act not only as a lipophilic prodrug of the nucleoside monophosphate but also a lipophilic prodrug of the combined 5',5'-dinucleoside monophosphate, and (iv) the triesters function as "depot forms" for the parent nucleosides. Additionally, cordycepin was chosen for an expected synergistic effect[11] due to its antibiotic activity and, as a nucleoside, could be easily introduced into the phosphotriester system with the same chemistry as for AZT.

A similar approach to phosphotriester derivatives of antiviral nucleosides bearing two alkyl chains[20-22] or one phenolic residue with two identical antiviral (HSV) nucleosides was described recently.[23] The validity of the phosphotriester approach was recently demonstrated by biodegradation assays in vivo[24] and in vitro.[12,25]

Chemistry

Recently, we published a new efficient synthesis for 3'-deoxyadenosine (**3**, cordycepin) starting from adenosine in an overall yield of 56%.[26] Before introducing **3** into the triesters **2a** and **2b**, we needed 2',N^6-dibenzoyl-3'-deoxyadenosine (**4**) as a protected derivative of **3**. Scheme II shows the five-step synthetic pathway starting from **3** to give **4** as a crystalline, colorless product in an overall yield of 65%. The critical step after perbenzoylation to **5** and selective debenzoylation[27] to **6** is the selective introduction of the 5'-*O*-dimethoxytrityl (DMTr) protecting group (step iii) which was carried out according to a published procedure.[28] It has to be noted that the substitution of the DIPEA by DMAP, or omission of these bases (only the solvent pyridine acting as base), resulted in a strong decrease in the yield of **7** because of formation of a mixture of **7**, the 5'-O,N^6-ditritylated derivative, and the N^6-monotritylated product. The target compound **4** was obtained after selective 2'-O-benzoylation of **7** (step iv) analogously to a described procedure (95%)[29] and quantitative acidic detritylation of **8** (Scheme II; overall yield 64%).

(19) Furman, P. A.; Fyfe, J. A.; St. Clair, M. H.; Weinhold, K.; Rideout, J. L.; Freeman, G. A.; Nusinoff-Lehrman, S.; Bolognesi, D. P.; Broder, S.; Mitsuya, H.; Barry, D. W. *Proc. Natl. Acad. Sci. U.S.A.* **1986**, *83*, 8333.

(20) McGuignan, C.; Tollerfield, S. M.; Riley, P. A. *Nucleic Acids Res.* **1989**, *17*, 6065.

(21) McGuignan, C.; Shackleton, J. M.; Tollerfield, S. M.; Riley, P. A. *Nucleic Acids Res.* **1989**, *17*, 10171.

(22) A phosphoramidate triester with two alkyl chains and the anti cancer agent araC were described very recently: McGuignan, C.; Jones, B. C. N. M.; Riley, P. A. *Bioorg. Med. Chem. Lett.* **1991**, *1*, 607. McGuignan, C.; Jones, B. C. N. M.; Devine, K. G.; Nicholls, S. R.; O'Connor, T. J.; Kinchington, D. *Bioorg. Med. Chem. Lett.* **1991**, *1*, 729.

(23) Farrow, S. N.; Jones, A. S.; Kumar, A.; Walker, R. T.; Balzarini, J.; De Clercq, E. *J. Med. Chem.* **1990**, *33*, 1400.

(24) Namane, A.; Gouyette, C., Fillion, M. P.; Fillion, G.; Huynh-Dinh, T. *J. Med. Chem.* **1992**, *35*, 3039.

(25) Puech, F.; Pompon, A.; Lefebvre, L.; Gosselin, G.; Imbach, J. L. *Bioorg. Med. Chem. Lett.* **1992**, *2*, 603.

(26) Meier, C.; Huynh-Dinh, T. *Synlett* **1991**, *2*, 227.

(27) Jones, R. A. In *Oligonucleotide Synthesis*; Gait, M. J., Ed.; IRL Press: Oxford/Washington, DC, 1984; p 24.

(28) Recently, P. Herderwijn described the 5'-O-protection of **3** with trityl chloride in the presence of DMAP at 50 °C with a yield of 85%. Under these conditions we isolated only 35% of the desired product **7**: Herderwijn, P.; Pauwels, R.; Baba, M.; Balzarini, J.; De Clercq, E. *J. Med. Chem.* **1987**, *30*, 2131.

(29) Matsuda, A. *Synthesis* **1986**, 385.

Scheme III[a]

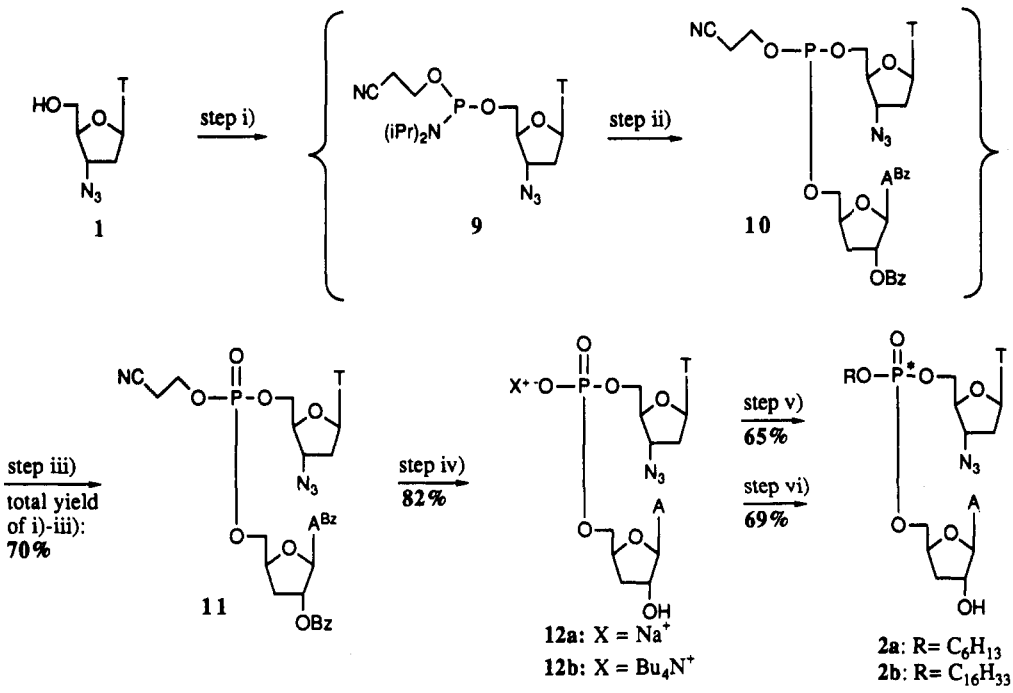

[a] Steps: (i) 1.1 equiv of $(NCCH_2CH_2O)(N(iPr)_2)PCl$, DIPEA, CH_3CN, 0 °C, 10 min; (ii) 4, tetrazole, CH_3CN, rt, 30 min; (iii) I_2, H_2O/THF/pyridine, rt, 5 min; (iv) (a) 1% NaOMe, MeOH, rt, 20 h; (b) Dowex H^+; (c) Dowex Bu_4N^+; (v) $C_6H_{13}I$, CH_3CN, 80 °C, 6 h; (vi) $C_{16}H_{33}I$, CH_3CN, 80 °C, 20 h.

The synthesis of the triesters **2a** and **2b** required two steps (Scheme III): (1) formation of the mixed nucleoside phosphodiester **12** and (2) its alkylation to yield **2a** and **2b**. The formation of the mixed nucleoside phosphodiester **12** was achieved by using phosphoamidite chemistry. AZT (1) was phosphitylated using β-(cyanoethyl)diisopropylchlorophosphoamidite to give **9**, which upon activation with tetrazole reacted with **4** to yield the dinucleoside phosphite **10**. Its oxidation under standard conditions gave the phosphotriester **11** in an overall yield of 70% (steps i–iii). Because of the great instability of the intermediates **9** and **10**, these steps were carried out as a one-pot reaction. Concerning step i, complete conversion could be ascertained after 10 min by TLC. Step ii was completed within 20 min. Interestingly, when we replaced β-(cyanoethyl)-diisopropylchlorophosphoramidite in step i by bis(diisopropyl)chlorophosphoramidite, no reaction took place. Changing the solvent from acetonitrile to diethyl ether or dichloromethane had no effect. By contrast, when we reacted bis(diisopropyl)chlorophosphoramidite with β-cyanoethanol in acetonitrile or dichloromethane, we observed the formation of the phosphitylated alcohol, and subsequent addition of AZT (1) under activation with diisopropylammonium tetrazolide yielded **9** within 10 min. Inversion of the reaction sequence, where 1 was added to the phosphitylated cordycepin derivative, did not give product **11**. The structure of **11** was confirmed by means of ^1H-, ^{13}C-, and ^{31}P-NMR as well as by the ^1H–^{13}C heteronuclear correlation.

Basic treatment of **11** gave, after neutralization and tetrabutylammonium Dowex ion exchange, the 5′,5′-linked dinucleoside phosphate diester **12** in 82% yield. The target triesters **2a** and **2b** were obtained as 1:1 mixtures of two diastereoisomers (R_p, S_p) from **12b** by direct nucleophilic displacement of 1-iodohexane (70%) and 1-iodohexadecane (60%) in boiling acetonitrile,[13,14] respectively. During the purification, we were able to isolate both diastereoisomers of **2a** and **2b** by silica gel chromatography, which were characterized by the means of ^1H-, ^{13}C-, and ^{31}P-NMR and COSY as well as by FAB-MS.

Table I. Partition Coefficient (PC) in Octanol/Water

compd	log PC[a]
AZT (1)	0.10[b]
cordycepin (3)	−0.65
diester **12a**	−1.33
triester **2a**	1.11
triester-**2b**$_R$	3.16
triester **2b**$_S$	3.26

[a] $PC = E_{octanol}/E_{water}$. [b] Reference 2.

Attempts to synthesize a phosphotriester with a methyl group as alkyl residue under the same conditions failed. NMR analysis of the reaction product showed a compound containing the *O*-methyl and the 5′-AZT moiety as well as a 5′-ribose residue but no signals of the purine heterocycle of cordycepin. Additional evidences for this depurinated product were the appearance of a second doublet resonance of the anomeric proton of the ribose ring (α,β mixture: δ 5.18 and 5.24 ppm) as well as a second set of ^{31}P-NMR resonances for the R_p,S_p phosphotriesters (α,β mixture: δ 0.13/0.25 and 0.25/0.38 ppm); this product was formed by alkylation at the N7 atom of the purine ring and subsequent breakage of the glycosidic bond.

During the purification and characterization of **2a** and **2b**, we observed a correlation between the mobility on silica gel and the chemical displacement in the ^{31}P-NMR spectra. The *fast* eluting diastereoisomers exhibited smaller δ values (**2a**$_R$ R_f 0.83; δ 0.85 ppm and **2b**$_R$ R_f 0.70; δ 0.88 ppm) with respect to the *slow* eluting diastereoisomers (**2a**$_S$ R_f 0.79; δ 0.91 ppm and **2b**$_S$ R_f 0.64; δ 0.97 ppm): by comparison of our data with the literature[30–33] we attributed the R_p configuration to the *fast* and the S_p configuration

(30) Potter, V. L.; Eckstein, F. *Nucl. Acids Res.* **1983**, *11*, 7087.
(31) Stec, W. J.; Zon, G.; Gallo, K. A., Byrd, R. A. *Tetrahedron Lett.* **1985**, *26*, 2191.
(32) Gallo, K. A., Shao, K.; Phillips, L.; Regan, J. B.; Koziolkiewicz, M.; Uznanski, B.; Stec, W. J.; Zon, G. *Nucl. Acids Res.* **1986**, *14*, 7405.
(33) Herding, W.; Seela, F. *J. Org. Chem.* **1985**, *50*, 5314.

Table II. Proton Chemical Shifts (in ppm from TSP) of $2b_R$ and $2b_S$ Solubilized in Deuteriated Dodecylphosphocholine Micelles at 20 °C

dA			AZT			alkyl chain		
	$2b_R$	$2b_S$		$2b_R$	$2b_S$		$2b_R$	$2b_S$
H8	8.18	8.23	H6	7.38	7.44	CH_2OP	4.01	4.04
H2	8.16	8.20	CH_3	1.74	1.80	CH_2CH_2OP	1.58	1.62
NH_2	6.95	6.95	H1′	6.08	6.06	$(CH_2)_{13}$	1.2	1.2
H1′	5.98	6.03	H2′	2.36	2.27	CH_3	0.78	0.78
H2′	4.66	4.72	H2″	2.44	2.44			
OH2′	6.67	6.68	H3′	4.39	4.31			
H3′	2.25	2.33	H4′	4.05	4.00			
H3″	2.12	2.20	H5′	4.27	4.27			
H4′	4.66	4.67	H5″	4.22	4.21			
H5′	4.41							
H5″	4.26	4.37						

to the *slow* migrating diastereoisomer. These attributions were further confirmed by an NMR structural analysis (see below).

Conformational and Biological Studies

Partition Coefficient. In order to measure the lipophilicity of phosphotriesters **2a** and **2b**, we determined their partition coefficients in water/octanol.[34] The concentrations were measured by means of UV data. Table I shows that both triesters are much more lipophilic than the parent compounds AZT (1) and 3′-deoxyadenosine (3), the phosphodiester **12a** being the most polar compound. Between **2a** and **2b** one can observe the expected difference in the partition coefficients correlated with the alkyl chain length. Additionally, **2a** as well as **2b** showed higher partition coefficient values than those previously described.[13] Only a small difference, not significant, was observed between the two diastereoisomers ($2b_S$ 3.26; $2b_R$ 3.16). On the other hand, we found no difference on the retention times for $2b_S$ and $2b_R$ on reversed-phase HPLC analysis (9.14 min).

Conformations of the Diastereoisomers. (a) Ab Initio Calculation. In order to evaluate the effect of different configurations at the phosphorus center of **2a** and **2b**, we carried out molecular-modeling calculations of both diastereoisomers of **2b**. Macromodel and the MM force field data were used for this studies.[36,37] In the energy minimization, the conformation of the glycosidic bond was shown to be anti for both nucleosides independent of the investigated diastereoisomer. The sugar puckering in cordycepin was the C2′-endo conformation whereas that in AZT was C3′-endo. Both structures found in the global energy minimum exhibited a gauche–gauche (gg) conformation of the C4′C5′ bond for AZT as well as for cordycepin. An important difference was found for the position of the nucleobases. In the S_p case we have found a base–base stacking of the two nucleosides with the alkyl chain pointing away. This conformation was ca. 10 kJ lower in energy than the following one. In contrast, in the R_p case, the situation is much more complicated: we have not found the base–base stacking but an interaction of thymine with the alkyl chain. Additionally, in this case the energy differences were small among several conformations. This result points out a much greater flexibility of the R_p molecule with regard to the S_p conformation.

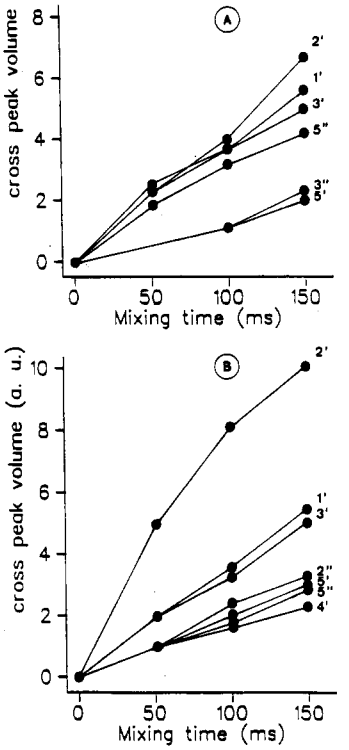

Figure 1. Build-up curves of the intranucleotide base-sugar proton-proton NOEs for $2b_R$ (20°C, D_2O solution). A) dA nucleotide; B) AZT nucleotide. The curve labeled 1′ corresponds to the H8(6)-H1′NOE, etc.

(b) NMR Conformational Studies in Deuteriated Dodecylphosphocholine Micelles. Each diastereoisomer $2b_R$ and $2b_S$ (determined as described in the previous paragraph) was solubilized with deuteriated dodecylphosphocholine micelles in aqueous solution at 20 °C. Under these experimental conditions, the corresponding 2D-NOESY spectra displayed numerous and intense cross peaks whereas similar experiments performed at the same frequency on free nucleotides gave weak or unobservable NOE correlations.[38] Three NOESY spectra were recorded with mixing times of 50, 100, and 150 ms. Figure 1 shows the plot of the base–sugar proton–proton NOE intensities versus mixing times for both nucleosides moieties of $2b_R$. These plots indicate that the buildup NOEs were still in the linear limit for a mixing time of 100 ms. In the following sections, NOE data were analyzed on the basis of 100-ms NOESY spectra.

Signal Assignment. Signal assignment was achieved from COSY and NOESY experiments. Since the two nucleoside sugars are chemically different, their corre-

(34) Rim, S.; Audus, K. L.; Borchardt, R. T. *Int. J. Pharm.* **1986**, *32*, 79. The partition coefficients were determined by UV spectroscopy at 265 nm.
(35) Kawaguchi, T.; Ishikawa, K.; Seki, T.; Juni, K. *J. Pharm. Sci.* **1990**, *79*, 531.
(36) Still, C. W. Program Macromodel V. 1.1, Columbia University, 1986.
(37) Burkert, U.; Allinger, N. L. *Molecular Mechanics*; ACS Monographs 177; American Chemical Society: Washington, DC, 1982.
(38) André, F.; Demassier, V.; Bloch, G.; Neumann, J. M. *J. Am. Chem. Soc.* **1990**, *112*, 6784.

sponding spin systems were readily identified in a COSY spectrum (not shown). Assignment of base and alkyl chain proton resonances was straightforward. The AZT H2′ and H2″ signals as well as the dA H3′ and H3″ signals were distinguished by comparing their NOE cross peaks: the H6(H8) base proton H2′(H3′) sugar proton NOE was markedly larger than the H6(H8) base proton H2″(H3″) sugar proton NOE (Figure 1). Proton chemical shifts of both diastereoisomers are listed in Table II.

Conformation of Nucleoside Moieties. In the proton spectrum of both diastereoisomers, the AZT H1′ signal exhibited a triplet structure with $J(1'2') = J(1'2'') = 6.5$ Hz. A similar spectral feature was observed for the free AZT nucleoside in aqueous solution and indicated a predominant C2′-endo conformation of the deoxyribose ring.[39] In regard to the distances between the deoxyribose protons and thus the corresponding NOEs, only the H2″–H4′ distance significantly varies according to the ring conformation (2.6 and 4.0 Å for the C3′-endo and C2′-endo conformers, respectively).[40] In agreement with the J values, a weak H2″–H4′ NOE corresponding to an interproton distance greater than 3.5 Å (i.e., consistent with a predominant C2′-endo conformation) was detected in both diastereoisomers' spectra. Lastly, the strong H6-H2′ NOE observed in both cases (see Figure 1B for $\mathbf{2b}_R$) is also indicative of a preferential C2′-endo conformer.

The dA H1′ signal of both diastereoisomers appeared as a singlet. Such a line structure revealed a weak value of the $J(1'2')$ coupling constant (<1 Hz) and therefore a large proportion of the C3′-endo conformation for the dA sugar ring. In the case of a 3′-deoxyribose, the H1′–H3″ distance is the most sensitive to the ring conformation (2.8 and 4.2 Å for the C2′-endo and C3′-endo conformers, respectively). The weak H1′–H3″ NOE found for both diastereoisomers is in favor of a preferential C3′-endo conformation.

Except for the dA sugar of $\mathbf{2b}_S$, the H5′ and H5″ signals of each sugar exocyclic groups gave discernible cross peaks. In all cases, the intensity of the H5′–H4′ NOE was quite close to that of the H5′–H4′ NOE. This result indicates a large proportion of the gauche–gauche conformation around the C4′–C5′ bond since, for the two other staggered rotamers, one of the NOEs is about 3.5 times greater than the other.

The base orientation around the glycosidic bond (defined by the χ angle C2–N1–C1′–O4′ (AZT) or C4–N9–C1′–O4′(dA)) was investigated from the intranucleotide H6(H8)–sugar proton NOE pattern. The base–sugar NOE pattern relative to $\mathbf{2b}_R$ is shown in Figure 1 and was found to be nearly identical to that of $\mathbf{2b}_S$ (not shown). Taking into account the preferential sugar conformation of the AZT and dA moieties, the NOE patterns of AZT H6 and H8 protons are consistent with a predominant anti orientation of the base (χ values ranged between −170° and −90°). However, the (H6(H8)–H5′ NOE)/(H6(H8)–H5″ NOE) intensity ratio differed between AZT and dA. In the former case, this ratio is close to 1 and thus is consistent with χ values around −130°. In the latter case, one of the NOEs was about two times greater than the other, and this discrepancy indicates a predominant anti orientation close to the extreme χ value of −170°. Such a difference was also revealed by the presence of a significant AZT H6–H4′ NOE whereas the dA H8–H4′ NOE is hardly discernible.

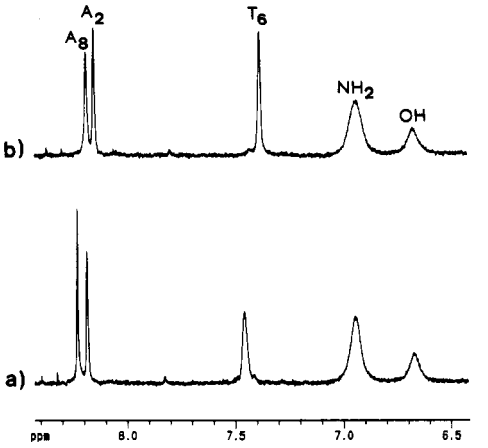

Figure 2. 8.5-6.5 ppm region of the 500 MHz spectra (H_2O:D_2O, 90:10 at 20°C) of $\mathbf{2b}_S$ (a) and $\mathbf{2b}_R$ (b), A8, A2 and T6 refer to the dA, H8, dA H2 and AZT H6 protons. The signals labeled NH_2 and OH correspond to the adenine amino protons and the dA 2′hydroxy proton respectively.

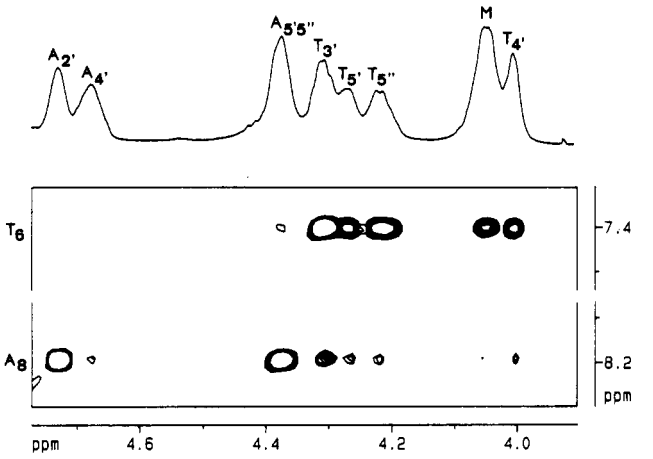

Figure 3. Region of the $\mathbf{2b}_S$ 500 MHz NOESY spectrum (D_2O solution at 20°C, mixing time: 100 ms) containing cross peaks connected to the H6(AZT) and H8(dA) resonances. The resonances are labeled as in figure 2. The signal labeled M corresponds to the first methylene protons of the alkyl chain.

Relative Orientation of the AZT, dA, and Alkyl Chain Moieties. The chemical shift analysis provided preliminary information about the orientation of the various moieties. For both diastereoisomers, the resonance of the H8 adenine proton (δ = 8.2 ppm, Table II) was dramatically shifted upfield from that observed in the free dA nucleotide (δ = 8.4 ppm).[41] In contrast, no significant difference was found for the other adenine protons (H2 and NH_2).

Additional information was obtained from the signal line widths which revealed a diastereoisomeric effect. In the case of $\mathbf{2b}_S$ (Figure 2a), the thymine H6 resonance is markedly broader than the other aromatic signals. After subtracting the $J(6\text{-}CH_3)$ coupling constant (1.5 Hz), the H6 line width was found to be around three times larger than the H8 one. In contrast, the aromatic resonances of $\mathbf{2b}_R$ (Figure 2b) exhibited similar line widths.

Lastly, direct conformational data were derived from proton–proton NOEs observed between the various moieties. As for the line widths of the aromatic protons, a dramatic difference was found between the diastereoisomers since only the $\mathbf{2b}_S$ NOESY spectrum displayed significant intermoiety contacts. Figure 3 shows the region

(39) Swapna, G. V. T.; Jagannadh, B.; Gurjar, M. K.; Kunwar, A. C. *Biochem. Biophys. Res. Commun.* **1989**, *164*, 1086.
(40) Wüthrich, K. *NMR of proteins and nucleic acids*; J. Wiley and Sons: New York, 1986.
(41) Bazin, H.; Chattopadhyaya, J. *Synthesis* **1985**, 1108.

of the $2b_S$ NOESY spectrum containing a well-defined cross peak between the adenine H8 signal and the AZT H3' signal. Weaker H8(dA)–H4', –H5', and H5''(AZT) correlations were also detected. Furthermore, the H6 and CH_3 AZT resonances showed strong NOEs to the CH_2OP and CH_2CH_2OP signals of the alkyl chain. The H6-CH_2OP cross peak is shown in Figure 3. NOESY spectra recorded in a H_2O/D_2O 90/10 solution did not provide any additional information.

Conformation of $2b_S$ in Micelles. The AZT–alkyl chain NOE's clearly revealed that the thymine base of $2b_S$ is embedded in the hydrophobic core of the micelle. This can be readily related to the large H6 line width previously mentioned. The location of the thymine base inside the micelle implies that the sugar ring roughly lies parallel to the micelle surface and thus orients the azido group toward the aqueous medium. Therefore, the NOE observed between the AZT H3' signal and the H8 dA signal suggests a close proximity between the azido group and the adenine five-membered ring.

Considering the electronic structure of the azido group, such a proximity explains the unusual upfield chemical shift of the H8 resonance at 8.23 ppm. Since the $2b_S$ H8 signal is located upfield with respect to the H8 resonance of the free dA nucleotide, one can reasonably conclude that the adenine and the azido group are coplanar and exhibit a particular local interaction.

Conformation of $2b_R$ in Micelles. The Diastereoisomeric Effect. In the case of $2b_R$, the lack of significant intermoiety NOEs precluded any global conformational description. Furthermore, as revealed by the line width analysis, none of the two nucleotide bases of $2b_R$ is buried in the hydrophobic core of the micelle and thus the conformational flexibility of this molecule is expected to be greater than that of $2b_S$. However, the adenine H8 resonance of $2b_R$ exhibited the same unusual chemical shift as that observed for $2b_S$ which was explained by the proximity between the adenine and the azido group. Therefore, we may assume that a local azido-adenine interaction exists for both molecules and was not directly observed in the $2b_R$ spectra because of large conformational fluctuations. On the basis of this hypothesis, we were able to understand the diastereoisomeric effect from the following structural considerations.

Molecular models of the *R* and *S* diastereoisomers were generated using the Alchemy software. The AZT conformation was designed with a χ value of –130° for the base orientation, a C2'-endo conformer for the sugar ring, and a gg conformation around the C4'–C5' bond. A χ value of –170°, a C3'-endo conformer, and a gg rotamer were used for the dA conformation. In the case of the *S* diastereoisomer, we easily found a structure consistent with the dA–AZT NOE and AZT–alkyl chain NOE constraints (Figure 4). In contrast, we could not obtain an *R* diastereoisomeric conformation satisfying both NOE constraint sets, taking into account that the adenine base is not buried in the micelle. Since the embedding of the thymine base in the hydrophobic core of the micelle (revealed by the thymine–alkyl chain NOEs) was only observed for one diastereoisomer, we tentatively assign the $2b_S$ as the *S* isomer. Assuming that the azido group–adenine base interaction occurs for both diastereoisomers as indicated by our experimental data, we suggest that the *R* conformation is close to the *S* conformation described in Figure 4 except for the location of the P=O and alkyl chain ligands which are inverted. Therefore, the diastereoisomeric effect is explained as follows: in one case (*S*), the thymine base is close to the alkyl chain and thus buried in the micelle, whereas in the other case (*R*) the thymine base is close to the P=O bond. This NMR study clearly shows the stereospecific influence of a membrane-like environment on molecular structures.

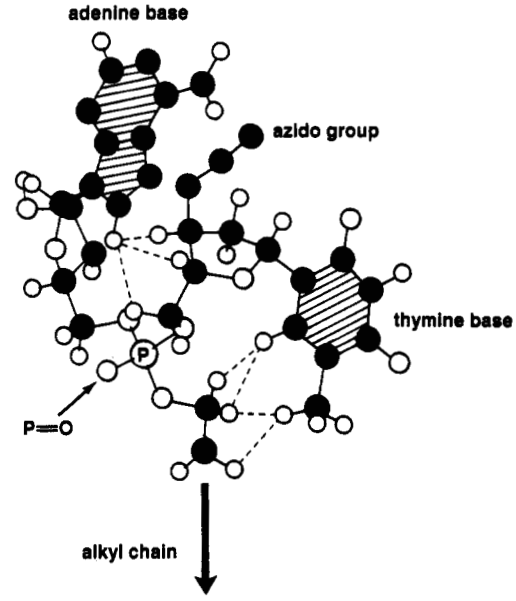

Figure 4. Molecular modeling of $2b_S$. Filled circles represent N and C atoms. Opened circles represent O and H atoms. The phosphorus atom is labeled with P. Dotted lines indicate the inter-moiety proton-proton NOEs.

Hydrolysis Study. The hydrolysis of the diastereoisomeric mixtures of **2b** was studied using buffered aqueous solutions adjusted at pH 1, 5, 7, and 10. For identification of the possible hydrolysis products we synthesized the corresponding nucleoside monophosphates of **1** and **3** as well as the two phosphodiesters **13** and **14** containing the hexadecyl chain and the 5'-linked nucleosides using the same procedure described for the synthesis of the mixed phosphodiester **12**. The hydrolysis studies were carried out at 37 °C, and aliquots of the mixtures were analyzed by HPLC. At pH 1, 5, and 7 no decomposition was observed over 21 days. In contrast, at pH 10 we observed a slow cleavage of the hexadecyl chain from **2b** resulting in the liberation of the mixed phosphodiester **12**.

Antiviral Activity. The antiviral activity of phosphodiester **12a** and phosphotriesters **2a**, $2b_R$, and $2b_S$ was measured on two lymphocytic cell lines (CEM-c113 and H9) infected with HIV-1 (Lai strain). To evaluate the antiviral activity of these compounds we studied (i) inhibition of the HIV-1 induced cytopathic effect (CPE) using the MTT cell viability to determine the CD_{50} and ED_{50CPE} and (ii) the reverse transcriptase (RT) activity in culture supernatants that determine the ED_{50RT}.

At day 7 postinfection, AZT the reference compound exhibited the same cytotoxicity and antiviral activity (CD_{50}: 10 μM, ED_{50RT}: 0.003 μM) in c113 and H9 cells. The ED_{50} values measured between day 7 and day 15 postinfection in both cell types decreased by 2 logs (0.2 and 0.5 μM respectively). The phosphodiester **12a** and the mixture of diastereoisomers of phosphotriesters **2a**, $2b_S$, and $2b_R$ displayed various patterns of toxicity. At doses up to 25 μM, as reported in Table III compounds **2a** and $2b_S$ displayed no toxicity for c113 cells. The data also show that these compounds are at least 2.5–15 times less toxic than AZT (CD_{50}: 150 and 19 versus 10 μM), diastereoisomer $2b_R$, and the phosphodiester **12a** (CD_{50}: 6.2 and 10 μM). The ED_{50RT} values for **2a**, $2b_R$, $2b_S$, and **12a** were all in the range of 1–2.5 μM giving selectivity indices (SI_{RT}) of 56, 2.5, 15, and 2000, respectively. In our series of

Table III. Comparative in Vitro Anti-HIV Efficacy and Cellular Toxicity of Phosphotriester and Phosphodiester Compounds

compd	cell type	day	CD_{50},[a] μM	ED_{50RT},[b] μM	ED_{50CPE},[c] μM	SI_{RT}[d]	SI_{CPE}[d]
2a	c113	7	150	2.25	125	56	1
2b$_R$	c113	7	6.2	2.5	5	2.5	1
2b$_S$	c113	7	19	1.25	10	15	2
12a	c113	7	10	0.005	0.05	2000	2000
		11	5	0.3	0.02	17	25
		15	5	1	2	5	2.5
12a	H9*	7	10	0.008	ND	1250	ND
		11	10	0.5	ND	20	ND
		15	10	2.6	ND	5	ND
AZT	c113	7	10	0.003	0.003	3000	3000
		11	5.6	0.03	0.008	167	625
		15	5.6	0.2	0.08	25	62
	H9*	7	10	0.003	ND	3000	ND
		11	10	0.5	ND	20	ND
		15	10	0.5	ND	20	ND

* H9 cells are not sensitive to the HIV-induced cytopathic effect. [a] CD_{50} concentration inducing 50% cell viability inhibition measured by the MTT method in C113 and H9 cells after 7, 11, and 15 days. [b] ED_{50RT} effective antiviral concentration producing 50% reduction of reverse transcriptase production in supernatant (measured by the RT method) of c113 and H9 cells after 7, 11, and 15 days. [c] ED_{50CPE} effective antiviral concentration producing 50% reduction of HIV-induced cytopathic effect measured by the MTT method in c113 and H9 cells after 7 and 15 days. [d] SI_{RT} and SI_{CPE} = selectivity index ratio CD_{50}/ED_{50} HIV-1 induced cytopathic effect or reverse transcriptase.

compounds only **12a** exhibited an SI similar to that of AZT for c113 or H9 cells at day 7 postinfection. At 11 and 15 days incubation, the selectivity indices values (SI_{RT}) for both compounds decreased by 2 or 3 logs for **12a** and 1 or 2 logs for AZT to SI_{RT} = 20 or 5 μM and 167 or 20 μM, respectively. All the compounds except **2a** significantly inhibited the HIV-1-induced cytopathic effect (ED_{50CPE}) by 5–10 μM for **2b$_R$** and **2b$_S$** and 0.005 μM for **12a**. Therefore, a large difference in activity was observed in regard to the ability to inhibit the HIV-1-induced cytopathic effect between for the mixture of the phosphotriesters **2a**, **2b$_S$**, and **2b$_R$** and the phosphodiester **12a** or AZT. Again, **12a** was more active than **2b$_R$**, **2b$_S$**, and **2a**; it displayed up to 3 logs of activity (SI_{RT} = 2000 versus 1 or 2) at a level similar to that of the reference compound AZT.

Conclusion

We have synthesized two different lipophilic phosphotriester derivatives as combined prodrugs for antiviral and antibiotic nucleosides. During the purification of one series of phosphotriester, we were able to separate the two diastereoisomers formed in the reaction in a ratio of 1:1. This allowed us to study their physical and conformational features in solution as well as their antiviral behavior. The ab initio molecular modeling of the conformation of the two diastereoisomers **2b$_R$** and **2b$_S$** shows the limits of this type of calculations since the *calculated* conformations of the sugar puckering and the base stacking could not be correlated with the *observed* conformations of these molecules in solution. Although the exact configuration at the P center could be deduced from their chromatographic mobility or their comparative ^{31}P chemical displacement, the NMR study of the conformation of these two diastereoisomers at the water-micelle interface brings an absolute proof of the chirality: due to the anchoring of the lipidic chain at the hydrophobic core of the micelle, the two diastereoisomers present different conformations as shown by the thymine interactions with the chain (in the *S* stereoisomer) or with the P=O bond (*R* stereoisomer). The two different behaviors of diastereoisomer **2b$_R$** and **2b$_S$** are also reflected in their antiviral activity: they presented different cytotoxicity and cytopathic effects, the *S* isomer giving the better selectivity index. We find again a high selectivity index[16] for the precursor phosphodiester **12**, as compared to the phosphotriesters **2a** and **2b**, in the in vitro test. The synergistic effect of the combination of the antibiotic cordycepin could not be demonstrated in these in vitro models.

In conclusion, the main interest of this work relies in the synthesis of a lipophilic phosphotriester combining two different nucleosides, the separation of the two diastereoisomers permitting the study of their physical and antiviral properties, as well as the different conformations of these compounds at a water–micelle interface by NMR spectroscopy.

Experimental Section

Dichloromethane was distilled from sodium carbonate; pyridine was twice distilled from calcium hydride and *p*-tolylsulfonylchloride; acetonitrile was distilled from phosphorous pentoxide. All reagents were used at the highest purity grade available. AZT was purchased from Sigma Chemicals, OH. β-(Cyanoethyl)-*N*,*N*-diisopropylchlorophosphoramidite was purchased from Aldrich Chemicals. Merck silica gel plates (60 F_{254}) were used for analytical TLC, and the spots were examined with UV light and anisaldehyde–sulfuric acid spray.

Mass spectra were obtained with a Varian MAT 711 instrument. Analytical HPLC was performed on a Hewlett–Packard 1090 M series, equipped with a diode-array detector and a Nucleosil C18 (5-mm) column, with gradients of acetonitrile in 0.01 M triethylammonium acetate (pH 7.0). UV spectroscopy was carried out using a Perkin-Elmer 550S spectrophotometer. Column chromatography was carried out on 230–400-mesh Merck silica gel. Some chromatographic purifications were done on a Chromatotron, Harrison Research Ltd., using plates prepared from silica gel Merck 60 PF_{254} type 7749.

For the NMR structural analysis, the phosphotriester molecules were dissolved in D_2O. Proton spectra (300 MHz), carbon spectra (75 MHz), and phosphorus spectra (121 MHz) were recorded on a Bruker AC 300 spectrometer and referenced to internal tetramethylsilane and 85% phosphoric acid, respectively.

N^6-Benzoyl-3′-deoxyadenosine (6). **6** was prepared analogously to a procedure previously described by Gait[27] starting from 3′-deoxyadenosine **3**[26] via the perbenzoylated product **5** [^1H NMR (DMSO-d_6) δ 2.47 (dd, 1 H, J = 13.94, 5.39 Hz), 2.96 (ddd, 1 H, J = 13.99, 10.72, 5.96 Hz), 4.61 (dd, 1 H, J = 12.20, 5.69 Hz), 4.71 (dd, 1 H, J = 12.20, 2.89 Hz), 4.89 (mc, 1 H), 6.04 (d, 1 H, J = 5.56 Hz), 6.27 (s, 1 H), 7.36 (t, 4 H, J = 7.52 Hz), 7.38 (t, 2 H, J = 7.82 Hz), 7.48 (mc, 4 H), 7.54 (d, 2 H, J = 7.43 Hz), 7.62 (t, 1 H, J = 7.43 Hz), 7.86 (d, 2 H, J = 7.47 Hz), 8.00 (d, 1 H, J = 7.44 Hz), 8.07 (d, 1 H, J = 7.46 Hz), 8.26 (s, 1 H), 8.57 (s, 1 H)] and selective debenzoylation reaction sequence: R_f 0.83 (dichloromethane/methanol (8.5:1.5)); ^1H NMR (DMSO-d_6) δ 1.96 (ddd, 1 H, J = 13.02, 6.07, 2.58 Hz), 2.29 (ddd, 1 H, J = 13.01, 7.81, 4.06 Hz), 3.38 (s (broad), 1 H, exchangeable), 3.55 (dd, 1 H, J = 12.01, 3.87 Hz), 3.73 (dd, 1 H, J = 12.03, 3.27 Hz), 4.41 (mc,

1 H), 4.65 (mc, 1 H), 5.15 (s (broad), 1 H, exchangeable), 6.04 (d, 1 H, J = 1.86 Hz), 7.55 (t, 2 H, J = 7.11 Hz), 7.65 (t, 1 H, J = 7.30 Hz), 8.05 (d, 2 H, J = 7.14 Hz), 8.74 (s, 1 H), 8.76 (s, 1 H), 11.24 (s (broad), 1 H, exchangeable).

N^6-Benzoyl-5′-(dimethoxytrityl)-3′-deoxyadenosine (7). N-Benzoylated cordycepin **6** (700 mg, 1.97 mmol) was twice coevaporated with 5 mL of pyridine. A solution of **6** in 10 mL of pyridine was stirred in the presence of diisopropylethylamine (280.0 mg, 2.17 mmol), (dimethylamino)pyridine (48.1 mg, 0.39 mmol), and dimethoxytrityl chloride (800.4 mg, 2.37 mmol) for 4 h at room temperature. After evaporation of the solvent and Chromatotron purification on silica gel, 1.08 g of **7** (84%) was isolated as a yellow foam: R_f 0.73 (dichloromethane/methanol (9:1)); ^{1}H NMR ($CDCl_3$) δ 2.16 (mc, 1 H), 2.30 (ddd, 1 H, J = 13.61, 7.08, 6.50 Hz), 3.28 (dd, 1 H, J = 10.51, 4.44 Hz), 3.40 (dd, 1 H, J = 10.58, 3.22 Hz), 3.75 (s, 6 H), 4.23 (s (broad), 1 H, exchangeable), 4.67 (mc, 1 H), 4.87 (mc, 1 H), 5.40 (s (broad), 1 H, exchangeable), 6.01 (d, 1 H, J = 1.66 Hz), 6.77 (d, 4 H, J = 8.81 Hz), 7.16 (d, 4 H, J = 8.85 Hz), 7.27 (mc, 5 H), 7.48 (t, 2 H, J = 7.76 Hz), 7.57 (t, 1 H, J = 7.54 Hz), 7.99 (d, 2 H, J = 7.30 Hz), 8.28 (s, 1 H), 8.58 (s, 1 H).

N^6,$O^{2'}$-Dibenzoyl-5′-(dimethoxytrityl)-3′-deoxyadenosine (8). **8** was synthesized analogously to a published procedure.[28] Tritylated **7** (903 mg, 1.37 mmol) was dissolved in 20 mL of dry acetonitrile. To this solution were added benzoic acid anhydride (372.8 mg, 1.64 mmol), (dimethylamino)pyridine (12.8 mg, 0.1 mmol), and triethylamine (180.4 mg, 1.78 mmol), and the solution was stirred for 1.5 h at room temperature to yield, after chromatographic purification, 1.1 g of **8** (99%) as a pale yellow foam: R_f 0.85 (dichloromethane/methanol (9.5:0.5)); UV (MeOH) 280 (22 500); ^{1}H NMR ($CDCl_3$) δ 2.38 (mc, 1 H), 3.05 (mc, 1 H), 3.45 (mc, 2 H), 3.79 (s, 6 H), 4.70 (mc, 1 H), 5.84 (mc, 1 H), 6.35 (d, 1 H, J = 1.45 Hz), 6.82 (d, 4 H, J = 8.90 Hz), 7.17 (d, 4 H, J = 8.86 Hz), 7.27 (mc, 5 H), 7.51 (mc, 6 H), 8.04 (mc, 4 H), 8.24 (s, 1 H), 8.81 (s, 1 H), 9.07 (s (broad), 1 H, exchangeable).

N^6,$O^{2'}$-Dibenzoyl-3′-deoxyadenosine (4). Compound **8** (1.00 g, 1.31 mmol) was treated with 60 mL of a 2% solution of benzenesulfonic acid (BSA) in dichloromethane/methanol (7:3) at 0 °C. After 15 min, no starting material could be detected by analytical TLC. Evaporation and purification by Chromatotron chromatography on silica gel yielded 597.7 mg of **4** (99%) as a colorless foam: R_f 0.65 (dichloromethane/methanol (9:1)); UV (MeOH) 280 (22 000); ^{1}H NMR ($CDCl_3$) δ 2.35 (ddd, 1 H, J = 14.00, 6.50, 3.20 Hz), 3.00 (ddd, 1 H, J = 14.00, 8.50, 6.47 Hz), 3.77 (dd, 1 H, J = 12.66, 2.22 Hz), 4.18 (dd, 1 H, J = 12.71, 1.67 Hz), 4.70 (dd, 1 H, J = 8.23, 6.67 Hz), 5.86 (dt, 1 H, J = 6.37, 3.23 Hz), 6.24 (d, 1 H, J = 2.64 Hz), 7.47 (t, 2 H, J = 7.42 Hz), 7.52 (t, 1 H, J = 7.73 Hz), 7.63 (mc, 2 H), 8.04 (d, 4 H, J = 8.07 Hz), 8.52 (s, 1 H), 8.81 (s, 1 H); HPLC min (99%); MS FAB$^-$ m/e 459 (M). Anal. ($C_{24}H_{21}N_5O_5$) C, H, N: calcd 62.71, 4.57, 15.24; found 62.59, 4.48, 15.09.

β-Cyanoethyl 3′-Azido-3′-deoxy-5′-thymidinyl N^6,$O^{2'}$-Dibenzoyl-3′-deoxy-5′-adenosinyl Phosphate (11). To an ice-cooled suspension of predried AZT (**1**, 158.8 mg, 0.59 mmol) in 4 mL of dry acetonitrile were added diisopropylethylamine (138.2 mg, 1.07 mmol), and β-cyanoethyldiisopropylchlorophosphoramidite (168.7 mg, 0.76 mmol) within 3 min at 0 °C. Approximately 2 min after addition of the phosphitylating agent a clear, colorless solution had been formed which was stirred for 10 min at 0 °C. Within this time TLC controls (ethyl acetate/petroleum ether (3:1)) showed complete conversion of **1** into **9** (R_f(**1**) 0.05; R_f(**9**) 0.65). To the solution of **9** was added a mixture of tetrazole (224.0 mg, 3.19 mmol) and dibenzoylated cordycepin **4** (210.0 mg, 0.45 mmol) in 2 mL of acetonitrile and the solution stirred at room temperature. Again, TLC controls showed complete conversion of **9** into **10** (dichloromethane/methanol (9:1), R_f(**10**) 0.55). **10** was directly oxidized by addition of 13 mL of the standard 0.1 M iodine reagent. After 30 min, the iodine excess was destroyed by addition of a concentrated solution of sodium hydrogen sulfite, the mixture was diluted with water, and the two phases were separated. The organic phase was extensively washed with water, dried over sodium sulfate, filtered, and evaporated to dryness. Chromatotron purification on silica gel gave 268.7 mg (70%) of the phosphotriester **11**: R_f 0.30 (dichloromethane/methanol (9:1)); ^{1}H NMR ($CDCl_3$) mixture of diastereoisomers δ 1.81 (s, 3 H), 2.38 (mc, 3 H), 2.76 (t, 2 H, J = 5.91 Hz), 2.89 (mc, 1 H), 3.95 (mc, 1 H), 4.35 (mc, 8 H), 4.79 (mc, 1 H), 6.01 (t, 1 H, J = 6.20 Hz), 6.05 (mc, 1 H), 6.35 (s, 1 H), 7.26 (s, 1 H), 7.47 (t, 4 H, J = 7.61 Hz), 7.56 (t, 1 H, J = 7.31 Hz), 7.61 (t, 1 H, J = 7.51 Hz), 8.05 (mc, 4 H), 8.37 (s, 0.5 H), 8.40 (0.5 H), 8.80 (s, 1 H); ^{13}C NMR ($CDCl_3$) mixture of diastereoisomers δ 12.25, 17.33, 18.63, 19.67 (2 × d, J = 2.26 Hz), 32.41, 32.53, 36.83, 42.82, 53.58, 54.58, 62.61 (2 × d, J = 4.52 Hz), 67.00, 68.36 (d, J = 5.10 Hz), 68.45 (d, J = 5.15 Hz), 78.14, 79.30 (2 × d, J = 7.42 Hz), 81.89 (d, J = 7.54 Hz), 85.65 (2 × s), 90.07 (2 × s), 111.31 (2 × s), 116.74, 123.75 (2 × s), 128.41, 128.52, 128.61, 128.78, 129.60 (2 × s), 132.71, 133.40 (2 × s), 133.82, 136.11 (2 × s), 142.29 (2 × s), 150.06, 150.57, 151.47, 152.42, 164.24, 165.64 (2 × s); ^{31}P NMR ($CDCl_3$) δ −3.55.

3′-Azido-3′-deoxy-5′-thymidinyl 3′-Deoxy-5′-adenosinyl Phosphate Sodium Salt (12a). **11** (250.0 mg, 0.29 mmol) was dissolved in 10 mL of a 1% solution of sodium methoxide in methanol and stirred at room temperature for 20 h. Neutralization of the resulting mixture with Dowex 50 WX8 (H^+ form), evaporation of the solvent, and washing the residue was dichloromethane left a colorless solid which was purified by chromatography on reversed-phase C18 silica gel using a gradient of water/acetonitrile. Subsequent cation exchange with Dowex 50 WX8 (Na^+ form) gave 160 mg (92%) **12a** as a colorless fluffy powder after lyophilization: HPLC 15.00 min (98.8%); UV (H_2O) 263 nm (18 000); ^{1}H NMR (D_2O) δ 1.68 (d, 3 H, J = 1.02 Hz), 2.19 (ddd, 1 H, J = 13.84, 6.15, 2.20 Hz), 2.38 (mc, 3 H), 4.08 (mc, 4 H), 4.21 (ddd, 1 H, J = 11.80, 3.97, 2.51 Hz), 4.38 (mc, 1 H), 4.72 (mc, 1 H), 4.83 (mc, 1 H), 6.08 (d, 1 H, J = 1.55 Hz), 6.13 (t, 1 H, J = 6.60 Hz), 7.46 (d, 1 H, J = 1.02 Hz), 8.36 (s, 1 H), 8.44 (s, 1 H); ^{13}C NMR (D_2O) δ 12.33, 33.71, 37.14, 53.44, 61.09, 66.16 (d, J = 5.12 Hz), 66.67 (d, J = 4.89 Hz), 76.20, 81.14 (d, J = 8.60 Hz), 83.62 (d, J = 9.04 Hz), 85.63, 91.91, 111.98, 119.26, 129.48, 130.12, 130.35, 138.03, 139.49, 143.10, 145.44, 148.66, 150.63, 152.12, 166.68; ^{31}P NMR (D_2O) δ 0.836. Anal. ($C_{20}H_{24}N_{10}O_9PNa$) C, H, N: calcd 39.86, 3.98, 23.25; found 39.98, 4.00, 23.17.

3′-Azido-3′-deoxy-5′-thymidinyl 3′-Deoxy-5′-adenosinyl Phosphate Tetrabutylammonium Salt (12b). The sodium salt **12a** was dissolved in water and passed through Dowex 50 WX8 tetrabutylammonium form. The appropriate fractions were lyophilized yielding **12b** quantitatively: UV (H_2O) 264 nm (20 000); ^{1}H NMR (D_2O) δ 0.91 (t, 12 H), 1.35 (sext, 8 H), 1.62 (mc, 8 H), 2.30 (mc, 4 H), 3.18 (mc, 4 H), 4.18 (mc, 1 H), 4.29 (mc, 1 H), 4.71 (mc, 1 H), 4.82 (mc, 1 H), 5.99 (d, 1 H, J = 1.45 Hz), 6.07 (t, 1 H, J = 6.55 Hz), 7.38 (d, 1 H, J = 0.88 Hz), 8.16 (s, 1 H), 8.24 (s, 1 H); ^{31}P NMR (D_2O) δ 0.87; ^{31}P NMR (MeOD) δ 2.18.

Hexyl 3′-Azido-3′-deoxy-5′-thymidinyl 3′-Deoxy-5′-adenosinyl Phosphate (2a). The tetrabutylammonium salt **12b** (85 mg, 0.103 mmol) was alkylated with 1-iodohexane (299.0 mg, 1.41 mmol) in 4 mL of acetonitrile overnight at 80 °C[13,14] to yield after purification by Chromatotron purification on silica gel[48] mg (70%) of phosphotriester **2a** as a 1:1 mixture of the two diastereoisomers: R_f 0.70 (R_p) and 0.64 (S_p) (dichloromethane/methanol (8:2)); HPLC 11.56 min (99%); MS FAB$^-$ m/e 664 (M); UV (octanol) 260 nm (19 000); ^{1}H NMR (MeOD) mixture of two diastereoisomers δ 0.88 (t, 3 H), 1.32 (mc, 6 H), 1.65 (mc, 2 H), 1.83 (2 × s, 3 H); 2.17 (mc, 1 H), 2.45 (mc, 3 H), 3.97 (mc, 1 H), 4.03 (2 × t, 2 H), 4.28 (mc, 4 H), 4.38 (mz, 1 H), 4.68 (mc, 1 H), 4.83 (mc, 1 H), 5.99 (d, 0.5 H, J = 1.54 Hz), 6.08 (d, 0.5 H, J = 1.60 Hz), 6.12 (t, 0.5 H, J = 6.60 Hz), 6.15 (t, 0.5 H, J = 6.60 Hz), 7.48 (s, 1 H); 8.20 (s, 1 H), 8.22 (s, 0.5 H), 8.25 (s, 0.5 H); ^{31}P NMR (MeOD) δ 0.857 (S_p), 0.914 (R_p). Anal. ($C_{26}H_{37}N_{10}O_9P$ C, H, N: calcd 46.97, 5.57, 21.08; found 46.81, 5.41, 46.97.

Hexadecanyl 3′-Azido-3′-deoxy-5′-thymidinyl 3′-Deoxy-5′-adenosinyl Phosphate (2b). The same procedure[13,14] using **12b** (57.3 mg, 0.07 mmol) and 1-iodohexadecane (298.7 mg, 0.85 mmol) was used as described for the synthesis of **2a**. After column chromatography on silica gel 34 mg (60%) of pure **2b** was isolated as a 1:1 mixture of the two diastereoisomers: R_f 0.83(R_p, fast) and 0.79 (S_p, slow) (dichloromethane/methanol (8:2)); HPLC 9.14 min (both diastereoisomers, 99.12%); MS FAB$^-$ m/e 804 (M); UV (octanol) 262 nm (19 000); ^{1}H NMR (MeOD, fast eluting diastereoisomer) δ 0.89 (t, 3 H, J = 7.01 Hz), 1.25 (mc, 26 H), 1.59 (q, 2 H, J = 6.90 Hz), 1.82 (d, 3 H, J = 1.00 Hz), 2.10 (ddd, 1 H, J = 13.38, 6.05, 2.28 Hz), 2.33 (ddd, 1 H, J = 13.38, 6.05, 2.28 Hz), 2.43 (ddd, 1 H, J = 13.90, 7.60, 6.10 Hz), 2.47 (ddd, 1 H, J = 13.92, 7.62, 6.09 Hz), 4.03 (dt, 1 H, J = 13.70, 6.60 Hz), 4.05 (dt, J = 13.71, 6.60 Hz), 4.29 (mc, 3 H), 4.42 (mc, 2 H), 4.71 (mc, 1 H),

4.79 (mc, 1 H), 6.00 (d, 1 H, J = 1.61 Hz), 6.09 (t, 1 H, J = 6.50 Hz), 7.45 (d, 1 H, J = 1.12 Hz), 8.20 (s, 1 H), 8.28 (s, 1 H); ^{1}H NMR (MeOD, slow eluting diastereoisomer) δ 0.89 (t, 3 H, J = 7.03 Hz), 1.25 (mc, 26 H), 1.58 (mc, 2 H), 1.78 (d, 3 H, J = 0.95 Hz), 2.15 (ddd, 1 H, J = 13.40, 5.90, 2.42 Hz), 2.40 (mc, 3 H), 4.02 (mc, 1 H), 4.07 (dt, 1 H, J = 13.75, 6.60 Hz), 4.30 (mc, 1 H), 4.62 (mc, 1 H), 4.82 (mc, 1 H), 6.02 (d, 1 H, J = 1.65 Hz), 6.17 (t, 1 H, J = 6.55 Hz), 7.48 (d, 1 H, J = 0.95 Hz), 8.20 (s, 1 H), 8.25 (s, 1 H); ^{1}H NMR of the mixture of diastereoisomers in DMDO-d_6 all signals were broad because of formation of micelles 5.78 (s (broad), 1 H, exchangeable, OH), 7.27 (s (broad), 2 H, exchangeable, $NH_{2adenine}$), 11.41 (s (broad), 1 H, exchangeable, $NH_{thymine}$); ^{13}C NMR (MeOD, fast eluting diastereoisomer) δ 12.51, 14.49, 23.74, 26.47, 30.18, 30.49, 30.60, 30.66, 30.75, 30.78, 30.79, 31.19, 31.28, 33.08, 34.73, 37.63, 54.79, 61.49, 67.99 (d, J = 5.65 Hz), 69.81 (d, J = 6.03 Hz), 69.98 (d, J = 6.18 Hz), 76.52, 80.39 (d, J = 7.54 Hz), 83.55 (d, J = 7.69 Hz), 87.14, 93.45, 111.77, 120.53, 138.23, 140.50, 150.12, 152.07, 153.33, 157.33, 166.32; ^{13}C NMR (MeOD, slow eluting diastereoisomer) δ 12.56, 14.47, 23.75, 26.49, 30.19, 30.49, 30.61, 30.67, 30.76, 30.80, 31.19, 31.28, 33.09, 34.99, 37.68, 54.79, 61.57, 68.20 (d, J = 5.73 Hz), 69.95 (d, J = 6.19 Hz), 76.47, 80.33 (d, J = 7.47 Hz), 83.48 (d, J = 7.69 Hz), 86.63, 93.35, 111.91, 120.52, 137.77, 140.52, 150.21, 152.11, 153.91, 157.33, 166.25; ^{31}P NMR (MeOD) fast eluting diastereoisomer δ 0.97, in $CDCl_3$ δ −2.34; ^{31}P NMR (MeOD) slow eluting diastereoisomer δ 0.885, in $CDCl_3$ δ −2.54. Anal. ($C_{36}H_{57}N_{10}O_9P$) C, H, N: calcd 53.73, 7.09, 17.41; found 53.59, 6.92, 17.26.

Attempts To Prepare Methyl 3′-Azido-3′-deoxy-5′-thymidinyl 3′-Deoxy-5′-adenosinyl Phosphate. The same procedure[13,14] using **12b** (57.3 mg, 0.07 mmol) and 1-iodomethane (298.7 mg, 3.14 mmol) was used as described for the synthesis of **2a**. After column chromatography on silica gel, a product (15 mg) was isolated and identified as a phosphotriester containing the methyl group as well as the AZT moiety but only a ribose residue: R_f 0.85 (dichloromethane/methanol (8:2)); ^{1}H NMR (MeOD) δ 1.92 (s, 3 H), 2.42 (t, 2 H), 3.85 (d, 3 H), 4.12 (mc, 5 H), 4.32 (mc, 3 H), 4.48 (mc, 2 H), 5.18 (d, 1 H), 6.21 (t, 1 H), 7.55 (s, 1 H); ^{31}P NMR (MeOD) two sets of diastereoisomers (R_p, S_p, α, β) δ 0.134, 0.252, 0.253, 0.382.

Hexadecyl 3′-Azido-3′-deoxy-5′-thymidinyl Phosphate Sodium Salt (13). **13** was prepared analogously as described for the dinucleoside phosphodiester **12a** via the corresponding β-(cyanoethyl)phosphotriester. After lyophilization **13** was obtained as a colorless powder in 60% yield: HPLC 7.53 min (97.8%); UV (H_2O) 268 nm (16 000); ^{1}H NMR (D_2O) δ 0.83 (t, 3 H, J = 7.05 Hz) 1.28 (mc, 26 H), 1.57 (q, 2 H, J = 6.75 Hz), 1.88 (d, 3 H, J = 1.00 Hz), 2.22 (mc, 2 H), 3.89 (mc, 2 H), 4.12 (mc, 3 H), 4.29 (mc, 1 H), 6.12 (t, 1 H, J = 6.45 Hz), 7.78 (d, 1 H, J = 1.00 Hz); ^{31}P NMR (DMSO-d_6) δ 0.348.

Hexadecyl 3′-Deoxy-5′-adenosinyl Phosphate Sodium Salt (14). **14** was synthesized as described for **13** and **12a**. It was obtained as a colorless powder after lyophilization: HPLC 5.28 min (98.8%); UV (H_2O) 260 nm (15 500); ^{1}H NMR (D_2O) δ 0.84 (t, 3 H, J = 6.95 Hz), 1.03 (mc, 26 H), 1.29 (mc, 2 H), 2.12 (mc, 1 H), 2.39 (mc, 1 H), 3.96 (mc, 2 H), 4.12 (mc, 1 H), 4.27 (mc, 1 H), 4.58 (mc, 1 H), 4.77 (mc, 1 H), 6.00 (s, 1 H), 8.11 (s, 1 H), 8.57 (s, 1 H); ^{31}P NMR (D_2O) δ 1.02.

NMR Experiments. A 5-mg portion of each diastereoisomer was cosolubilized with 32 mg of deuteriated dodecylphosphocholine (MSD Isotopes) in 0.5 mL of 10 mM phosphate buffer containing 0.1 mM EDTA and lyophilized in either D_2O or H_2O–D_2O (90:10). The pH was adjusted to 6.5. The solution was sonicated for 10 min with a Branson sonicator. A standard set of 500-MHz two-dimensional phase-sensitive experiments (COSY and NOESY)[40] was performed on a Bruker AMX 500 spectrometer at 20 °C. In general, a total of 48 (COSY) or 80 (NOESY) transients were acquired with a recycling delay of 1 s. A total of 512 increments of 2K data points were collected for each 2D experiment yielding a digital resolution of 6 or 8 Hz/point in both dimensions after zero filling. Shifted squared sine-bell functions were used for apodization. None of the 2D experiments was symmetrized. Three NOESY spectra were recorded with mixing times of 50, 100, and 150 ms. The Alchemy software (Tripos Ass.) was used for molecular modeling.

Antiviral Assay on CEM-c113 and H9 Cells. Compounds were tested and compared to AZT (obtained from Sigma) for cytotoxicity and ability to inhibit HIV replication. They were dissolved at 10 mM in either a 10:100 methanol–H_2O mixture or H_2O only. All compounds were diluted in phosphate-buffered saline (PBS) just before use. The HIV-1 induced cytopathic effect (CPE) was monitored by the MTT viability assay. To follow HIV replication (see below) we measured reverse transcriptase activity in the culture supernatant. Briefly, 125 μL of cell suspension (1 × 10^5 cells/mL) in RPMI-1640 medium supplemented with 10% fetal calf serum, 100 IU of penicillin per mL, 100 μg of streptomycin per mL, and 2 μg of polybrene per mL, was incubated in microtitration plates for 1 h with 25 μL of 10-fold diluted concentrations of the compounds. The CEM-c113 or H9 cells cultures were infected by the addition of 100 μL of HIV-1 (Lai Strain) containing 50–250 times the minimal necessary dose. Mock infected cells were treated with 100 μL of supplemented RPMI only. Cells were then incubated for 7 days at 37 °C in a CO_2 incubator (5%). At day 7 and then every 3 or 4 days 50 μL of the supernatant was removed for reverse transcriptase (RT) assay. Concomitantly, 100 μL of cell suspension was transferred into another microplate and mixed with 10 μL of the 3-(4,5-dimethylthiazol-2-yl)-2,5-diphenyltetrazolium bromide (MTT assay)[16] to determine cell viability. The percentage of toxicity of the products in these cells was defined in relation to the toxicity of uninfected untreated control cells.

Results were expressed according to the formula

$$\% \text{ viable cells} = \frac{\text{OD of treated} \pm \text{infected cells}}{\text{OD of mock} \bullet \text{infected cells}}$$

The 50% cytotoxic dose (CD_{50}) was defined as the concentration of compound that reduced the absorbance of the mock-infected control sample by 50%. The dose giving 50% protection was defined as the 50% effective dose (ED_{50}). The selectivity index is the ratio CD_{50}/ED_{50}.

Fresh medium (150 μL) with or without the compound tested was added to the cell suspension remaining in the original microplate for a longer incubation (>7 days). All assays were carried out in triplicate.

In Vitro Reverse Transcriptase Assay. The determination of reverse transcriptase activity was determined in cell supernatants as a marker of HIV replication, as previously described.[16] Briefly, 50 μL of supernatant was incubated for 1 h at 37 °C with 50 μL of buffer containing 50 mM Tris-HCl (pH 8), 50 mM KCl, 5 mM $MgCl_2$, 5 mM DTT, 0.5 mM EGTA, 0.05% Triton X-100, polyrA-oligoT 0.5 OD/mL, and ^{3}HdTTP 1 μCi. The polynucleotides were then precipitated with 20 μL of 60% trichloroacetic acid (TCA) in 120 mM $Na_4P_2O_7$, and the samples were filtered on glass fiber filters using a Skatron cell harvester. Filters were dried and counted in a 1240 rack Beta scintillation counter (LKB). Reverse transcriptase activity was expressed in counts per minute (cpm/min).

Results were expressed according to the formula

$$\% \text{ inhibition} = \frac{\text{cpm in treated infected cells (50 } \mu\text{L)}}{\text{cpm in infected cells (50 } \mu\text{L)}}$$

ED_{50RT} = dose giving 50% protection from HIV replication.

Acknowledgment. Our research was supported by the ANRS 90-91 program. We thank Professor J. Igolen for his support and encouragment. C.M. is grateful to the Fonds der Chemischen Industrie, Frankfurt/Main, Germany for a "Liebig Stipendium".

Supplementary Material Available: ^{1}H NMR spectra for compounds **2a**, **2b** (slow eluting diastereomer), **2b** (fast eluting diastereomer), **4**, **6**, **7**, **8**, **11**, **12b**, **12a**, **13**, and **14** (12 pages). This material is contained in many libraries on microfiche, immediately follows this article in the microfilm version of the journal, and can be ordered from the ACS; see any current masthead page for ordering information.